



AIIM

Association for Information and Image Management

1100 Wayne Avenue, Suite 1100

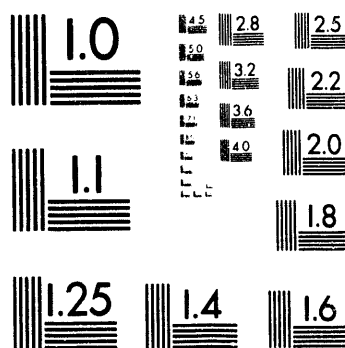
Silver Spring, Maryland 20910

301/587-8202

Centimeter



Inches



MANUFACTURED TO AIIM STANDARDS
BY APPLIED IMAGE, INC.

1 of 1

Global Coupling and Decoupling of the APS Storage Ring *

Y.C. Chae[†], J. Liu[‡], L. C. Teng
Argonne National Laboratory, 9700 So. Cass Ave., Argonne, 60439

Abstract

This paper describes a study of controlling the coupling between the horizontal and the vertical betatron oscillations in the 7-GeV Advanced Photon Source (APS) storage ring. First, we investigate the strengthening of coupling using two families of skew quadrupoles. Twenty skew quadrupoles are arranged in the 40 sectors of the storage ring and powered in such a way so as to generate both quadrature components of the required 21st harmonic. The numerical results from tracking a single particle are presented for the various configurations of skew quadrupoles. Second, we describe the global decoupling procedure to minimize the unwanted coupling effects. These are mainly due to the random roll errors of normal quadrupoles. It is shown that even with the rather large rms roll error of 2 mrad, the coupling effects can be compensated for with 20 skew quadrupoles each having maximum strength one order of magnitude lower than the typical normal quadrupole strength.

I. GLOBAL COUPLING

A. Introductory Remarks

For a given skew quadrupole distribution, $m(\theta) = \frac{1}{(B\theta)} \frac{\partial B_x}{\partial x}$, we can show that the ratio of the horizontal (x) and vertical (y) oscillation amplitude can be expressed as [1]

$$\frac{y_{amp}}{x_{amp}} \cong \frac{\frac{1}{2} \sqrt{a_k^2 + b_k^2}}{\nu_y^2 - (\nu_x - k)^2}, \quad (1)$$

where a_k and b_k are the k^{th} harmonic coefficients defined by

$$m(\theta) = \sum_{p=-\infty}^{p=+\infty} (a_p \cos p\theta + b_p \sin p\theta),$$

where θ is the azimuthal angle around the ring. Deriving Eq. (1), we assumed that the tunes are near the coupling resonance, namely, $|\nu_x - \nu_y| \cong k$. For the APS storage ring, since the design tunes are $\nu_x = 35.22$ and $\nu_y = 14.30$, the above equation clearly shows that we need to excite the $k = 21$ harmonic to cause the coupling most efficiently. In the next sections, the arrangement of skew quadrupoles to excite the 21st harmonic is discussed and some numerical results are presented.

B. Arrangement of Skew Quadrupoles

Consider N skew quadrupoles with the same strength evenly distributed around the ring with period $\frac{2\pi}{N}$ as shown in Fig. 1(a). Then Fourier harmonic numbers are $k = nN$ where n is an integer. In order to obtain the harmonic number k such that $k = nN + mM$, we may impose on top of Fig. 1(a) the square wave function with period $\frac{2\pi}{M}$. Such a function is shown in Fig. 1(b) and the corresponding modulated function can be

*Work supported by U.S. Department of Energy, Office of Basic Energy Sciences under Contract No. W-31-109-ENG-38.

[†]On leave from University of Houston.

[‡]On leave from University of Wisconsin, Madison.

expressed as a Fourier series by

$$f(\theta) = \frac{2N}{\pi^2} \sum_{m=1, \text{odd}} \frac{\sin(mM\theta)}{m} + \frac{2N}{\pi^2} \sum_{n=1} \sum_{m=1, \text{odd}} \frac{\sin(nN + mM)\theta - \sin(nN - mM)\theta}{m}. \quad (2)$$

Hence we show that we can generate an arbitrary harmonic by changing the period of the square wave function.

In the APS storage ring¹, the spaces available for the skew quadrupoles are between Q3 and S2 in the upstream half of a sector (half sector A), which we will call the A:QS family, and between Q4 and S3 in the downstream half of a sector (half sector B), which we will call the B:QS family. The number of skew quadrupoles considered is ten for each family. We may install the focusing A:QS in every fourth cell, say cell numbers 1, 5, 9, 13 and 17, and the defocusing A:QS in cells 21, 25, 29, 33 and 37. This family alone can adequately generate the desired 21st harmonic. Using Eq. (2), with $N = 10$ and $M = 1$ for the A:QS family, we find the coefficient of the 21st harmonic to be $b_{21} \equiv c = \frac{20}{\pi^2}$ which is greater than unity. The B:QS family adds to the quadrature components because A:QS and B:QS are not in phase. For the arrangement shown in Fig. 1(c) which we will call the "normal" arrangement, we may write

$$m(\theta) = c(a \cos 21\theta + b \sin 21\theta), \quad (3)$$

where $a = -\sin 21\Delta\theta_o$, $b = 1 + \cos 21\Delta\theta_o$, and $\Delta\theta_o$ is the shift of the origin of the B:QS family with respect to the origin of the A:QS family which is the middle of the A:QS skew quadrupole in cell number 1. In the APS storage ring $\Delta\theta_o$ is $\frac{\pi}{8}$. We note that, if A:QS and B:QS are exactly in phase, $a = 0$ and $b = 2$.

In the next section, we present numerical results of the coupling coefficient obtained by tracking a single particle. We first use the "normal" arrangement as the basis and then we attempt to find the optimum arrangement for obtaining full coupling.

C. Numerical Results

For single particle motion the Courant-Snyder invariant is

$$\epsilon_x = \frac{x^2 + (\alpha_x x + \beta_x x')^2}{\beta_x}.$$

The coupling ratio in this report is defined as

$$\kappa = \frac{(\epsilon_y)_{\text{max}}}{(\epsilon_x)_{\text{max}}}.$$

This definition is consistent with the ratio of emittances of a group of particles (a beam), because the emittance is the phase space area enclosed by the envelope of the beam. However, since the linear optical parameters, $\beta_{x,y}$ and $\alpha_{x,y}$, are ill-defined in the coupled lattice, our definition of the emittance is not the true projection of the four-dimensional phase space volume onto the (x, x') or (y, y') plane as defined in [3]. But for our application it is an adequate approximation to the real projected emittance.

¹For the arrangement of lattice elements and the nomenclature rules used in the APS project, see Ref. [2].

MASTER

DISTRIBUTION OF THIS DOCUMENT IS UNLIMITED

In order to estimate the coupling ratio with the intentional insertion of skew quadrupoles in the otherwise uncoupled APS storage ring lattice, we used the program MAD [4]. For “normal” configuration, we achieved full coupling with the integrated skew quadrupole strength of $B'l = 0.25$ T which is larger than the 0.2 T of the design normal operating strength.

In order to achieve full coupling at the skew quadrupole strength 0.2 T, we optimized the skew quadrupole arrangement. One optimization procedure is to rotate the B:QS family by $n \frac{2\pi}{10}$ in a clockwise direction while A:QS is fixed at the original place. With $n = 1$, B:QS in cell 3 goes to cell 7 and B:QS in cell 7 to cell 11 and so on. This operation is shown in Fig. 1(d). By using this shifting operation, we control the a and b coefficients in Eq. 3 which can be written

$$\begin{aligned} a &= a(A:QS) + a(B:QS), & b &= b(A:QS) + b(B:QS), \\ a(A:QS) &= 0, & b(A:QS) &= 1, \\ a(B:QS) &= -\sin 21\Delta\theta_n, & b(B:QS) &= \cos 21\Delta\theta_n, \end{aligned}$$

where $\Delta\theta_n = \Delta\theta_0 + \frac{2\pi}{10}n$ and $\Delta\theta_0 = \frac{\pi}{8}$. The coefficients $a(B:QS)$ and $b(B:QS)$ for different n values are plotted in the polar coordinate system as in Fig. 2. We notice that two skew families are almost in phase when $n = 7$ and the amplitude of the 21st harmonic is

$$|c_{21}| = \sqrt{a_{21}^2 + b_{21}^2} \cong 2,$$

which is the desired result.

The tune separation and the coupling ratio for various arrangements of the B:QS family of the skew quadrupoles with the integrated strength $B'l = 0.2$ T are listed in Table 1. The tune separation data, an indication of coupling, clearly shows that the $n = 7$ arrangement is the most efficient way of coupling the lattice. However, the coupling ratio doesn't show a clear advantage of the $n = 7$ over the $n = 8$ arrangement. This is because once the beam is close to full coupling, the coupling ratio is saturated, i.e. not much advantage is gained from the optimized arrangement over a less optimized one.

Table 1
Coupling Effects of Various Skew Quadrupoles
Arrangement

Arrangement No.	$ \nu_x - \nu_y $	$\kappa = \epsilon_{y\max}/\epsilon_{x\max}$
$n=0$ (normal)	0.104	0.797
$n=1$	0.080	0.403
$n=2$	0.087	0.542
$n=3$	0.115	0.798
$n=4$	0.145	0.891
$n=5$	0.171	0.888
$n=6$	0.185	0.936
$n=7$	0.186	0.952
$n=8$	0.172	0.963
$n=9$	0.145	0.936

II. GLOBAL DECOUPLING

A. Treatment of Weak Coupling Using Matrix Formalism

Following S. Peggs [5], we may write the normalized transfer matrix for the ring as

$$T = \begin{pmatrix} M & m \\ n & N \end{pmatrix}. \quad (4)$$

This normalized transfer matrix is the similarity transformation of the Edwards and Teng matrix [6], T' . We further define a “fundamental” coupling matrix as

$$H = m + n^+. \quad (5)$$

Then, on the coupling resonance $\nu_x = \nu_y$, the tune separation becomes

$$\delta\nu \cong \frac{\sqrt{\det(H)}}{2\pi\sin\pi(\nu_x + \nu_y)}. \quad (6)$$

The procedure to minimize $\delta\nu$ is often called “global decoupling.”

According to M. Billing [7], H can be written

$$H = H_+ \sin\pi(\nu_x + \nu_y) + H_- \sin\pi(\nu_x - \nu_y). \quad (7)$$

H_{\pm} are defined as

$$H_{\pm} = \sum_{SQ} q_m \begin{pmatrix} \cos\omega_{\pm}(s_m) & \sin\omega_{\pm}(s_m) \\ -\sin\omega_{\pm}(s_m) & \cos\omega_{\pm}(s_m) \end{pmatrix},$$

where $q_m = \frac{\sqrt{\beta_x \beta_y}}{f}$ is the dimensionless skew quadrupole strength of focal length f and

$$\omega_{\pm}(s_m) = (\pm\phi_y(s_m) - \phi_x(s_m)) + \pi(\pm\nu_y - \nu_x),$$

where $\phi_{x,y}(s_m)$ is the betatron phase at the skew quadrupole measured from the reference point. These expressions are convenient because all the quantities used in the formula are those of the uncoupled lattice. Defining $p = \sum q_m \cos\omega_+$ and $r = \sum q_m \sin\omega_+$, and noting that the contribution of the H_- term in Eq. (7) vanishes on the coupling resonance, we rewrite Eq. (6) as

$$\delta\nu = \frac{\sqrt{p^2 + r^2}}{2\pi}, \quad (8)$$

which we want to minimize.

B. Decoupling Procedure and Its Application

A routine procedure to decouple the lattice by the operator is simulated using the MAD program interactively. In the simulation, Q1s (see Ref. [2] for locations) are chosen as the trim quadrupoles.

Rewriting p and r ,

$$\begin{aligned} p &= \sum_{A:QS} q_m \cos\omega_+ \sum_{B:QS} q_m \cos\omega_+ + p_o \\ r &= \sum_{A:QS} q_m \sin\omega_+ \sum_{B:QS} q_m \sin\omega_+ + r_o \end{aligned} \quad (9)$$

where p_o and r_o are from the random roll errors of normal quadrupoles in the ring, we can see that it is convenient to use A:QS to control r , and B:QS to control p , or vice versa. With

the midpoint of the straight section of cell 0 as the reference point, we found that A:QS mainly controls τ . With the ten skew quadrupoles of the A:QS family, we get

$$p(A:QS) = 0.2 |q_m|, \quad r(A:QS) = 6.0 |q_m|.$$

For optimal control of p using the B:QS family, we consult Fig. 2 in order to find the most efficient arrangement. There we find that the phase of $n = 4$ or $n = 9$ arrangement is almost orthogonal to that of A:QS.

In the simulation, we used the $n = 0$ arrangement of B:QS. Coupling is caused by the random roll errors of normal quadrupoles. The minimum tune separations before and after decoupling are summarized in Table 2 with the same seed number for the assignment of random errors. We note that $\delta\nu$

Table 2
Effect of Decoupling Procedure on the Tunes

Error level	$\delta\nu$ (before)	$\delta\nu$ (after)	A:QS (B'l)	B:QS (B'l)
0.5 mrad	0.0186	0.00133	0.019 T	0.055 T
1.0 mrad	0.0353	0.00465	0.031 T	0.100 T
2.0 mrad	0.0714	0.0282	0.019 T	0.140 T

before decoupling is linearly proportional to the magnitude of rms errors, as expected.

The effects of decoupling on the phase motion at the normal tunes was found to reduce the coupling ratio significantly. For the error level of 2 mrad, the coupling ratio reduced down to 0.1 from 0.65.

III. CONCLUSION

In this report we investigated the coupling procedure to put a beam in the fully coupled state and the decoupling procedure to cancel the coupling effects due to the random roll errors of normal quadrupoles. The harmonic analysis of skew quadrupole distribution provides the common ground for finding the optimum arrangement of skew quadrupoles. We achieved full coupling at the integrated skew quadrupole strength of 0.2 T and we succeeded in reducing the coupling down to below 10 percent even with the rather large lattice quadrupole rms roll error of 2 mrad.

IV. REFERENCES

- [1] Y.C. Chae, "Global Coupling and Decoupling in the APS Storage Ring," ANL/APS/LS-207, May, 1992.
- [2] G. Decker, "Nomenclature and Name Assignment Rules for the APS Storage Ring," ANL/APS/LS-196, March, 1992.
- [3] K.L. Brown and R.V. Serfranckx, "Cross-Plane Coupling and Its Effects on Projected Emittance," SLAC-PUB-4679, August, 1989.
- [4] H. Grote and F.C. Iselin, "The MAD Program Version 8.1," CERN/SL/90-13(AP), May, 1990.
- [5] S. Peggs, "Coupling and Decoupling in Storage Rings," IEEE NS-30, No. 4, August, 1983.
- [6] D. Edwards and L.C. Teng, "Parameterization of Linear Coupled Motion in Periodic Systems," IEEE NS-30, No. 3, June, 1973.

[7] M. Billing, "Controls in Use at CESR for Adjusting Horizontal to Vertical Coupling," IEEE NS-32, No. 5, October, 1985.

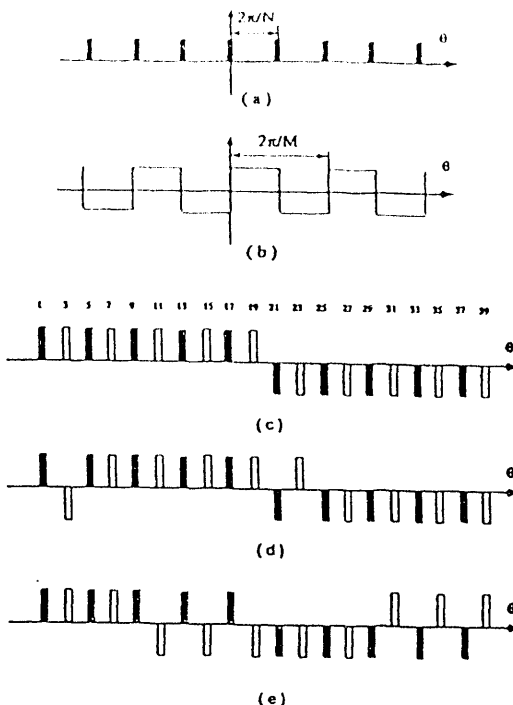


Figure 1

(a) Periodic delta function. (b) Square wave function. (c) Skew quadrupole arrangement where a solid block represents the A:QS family and a blank block represents the B:QS family. The number on the block indicates the cell number in the APS storage ring and we will call this arrangement the "normal" arrangement. (d) Shift of B:QS by an amount of $2\pi/10$, namely $n=1$. (e) Shift of B:QS by an amount $7\frac{2\pi}{10}$, namely $n=7$ (the optimized arrangement achieving full coupling).

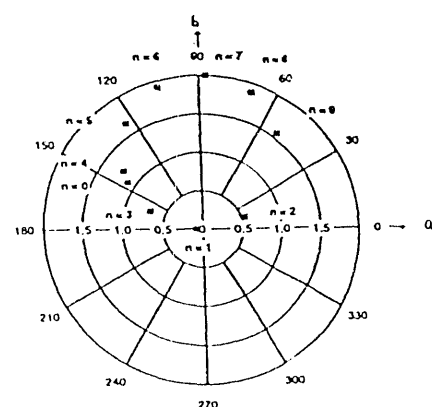


Figure 2

$a(B:QS)$ and $b(B:QS)$ coefficients from the B:QS skew quadrupole family. Note that since $a(A:QS)=0$ and $b(A:QS)\approx 1.0$, this figure shows that two families are almost in phase when $n=7$.

DISCLAIMER

This report was prepared as an account of work sponsored by an agency of the United States Government. Neither the United States Government nor any agency thereof, nor any of their employees, makes any warranty, express or implied, or assumes any legal liability or responsibility for the accuracy, completeness, or usefulness of any information, apparatus, product, or process disclosed, or represents that its use would not infringe privately owned rights. Reference herein to any specific commercial product, process, or service by trade name, trademark, manufacturer, or otherwise does not necessarily constitute or imply its endorsement, recommendation, or favoring by the United States Government or any agency thereof. The views and opinions of authors expressed herein do not necessarily state or reflect those of the United States Government or any agency thereof.

**DATE
FILMED**

9/21/93

END

